The value of a hole in coal:
Assessment of seasonal thermal energy storage and recovery in flooded mines

Abstract

Seasonal storage and extraction of waste heat in legacy coal mines could help decarbonize the space heating sector. The evolution of a mine-water thermal scheme is analyzed employing heat transport simulations in generic 3D conceptual models of a room-and-pillar extraction panel. We show that, by optimizing the seasonal management, up to 45% of the energy stored can be recovered (first year) in the modelled scheme. In favorable scenarios, the cumulative energy of the heat storage/extraction is equivalent to the energy provided by the mined coal in less than 80 years and its monetary worth could be achieved in less than 10 years; which evidences the value of legacy coal mines in the current energy context.

Keywords: geothermal, energy storage, energy value, groundwater, numerical modelling, coal mine

Authors:
Pérez, Jesus Alejandro [a*] - *perezsj.alejandro@gmail.com*
McDermott, Christopher [a] - *christopher.mcdermott@ed.ac.uk*

[a]*The University of Edinburgh, School of Geosciences, The King's Buildings, Edinburgh EH9 3FE, United Kingdom*
**Corresponding Author*

Abbreviations*:* BC, Boundary Condition; COP, Coefficient of Performance; CSR, Characteristic Sedimentary Rock; GSHP, Ground-Source Heat Pump; IC, Initial Condition.

1 - Introduction

The use of fossil fuels for space heating, a main CO_2 emission source in high-latitude regions (Watson et al., 2019; Sansom, 2014), constitutes a complex challenge for the ongoing energy transition given the characteristic high ramp-up rates and seasonal fluctuation in the demand (Figure 1). The heating and cooling sector, globally 51% of the total energy use (REN21, 2019), has not experienced the decarbonization witnessed in power generation with renewable sources of energy. Increasing the direct use of the low-enthalpy geothermal resource is being considered among other alternatives, such as green hydrogen and solar heating applications (Dodds & Demoullin, 2013; Dahash et al., 2019); to reduce the carbon intensity with district heating networks (Sayegh et al., 2017). A large-scale implementation of this option, however, has been mostly limited to tectonically active regions (Lund & Boyd, 2016) and its application is hindered by aspects such as the proximity of the resource to urban centers and adequate hydraulic conditions in the subsurface for open-loop systems (Bertermann et al., 2015).

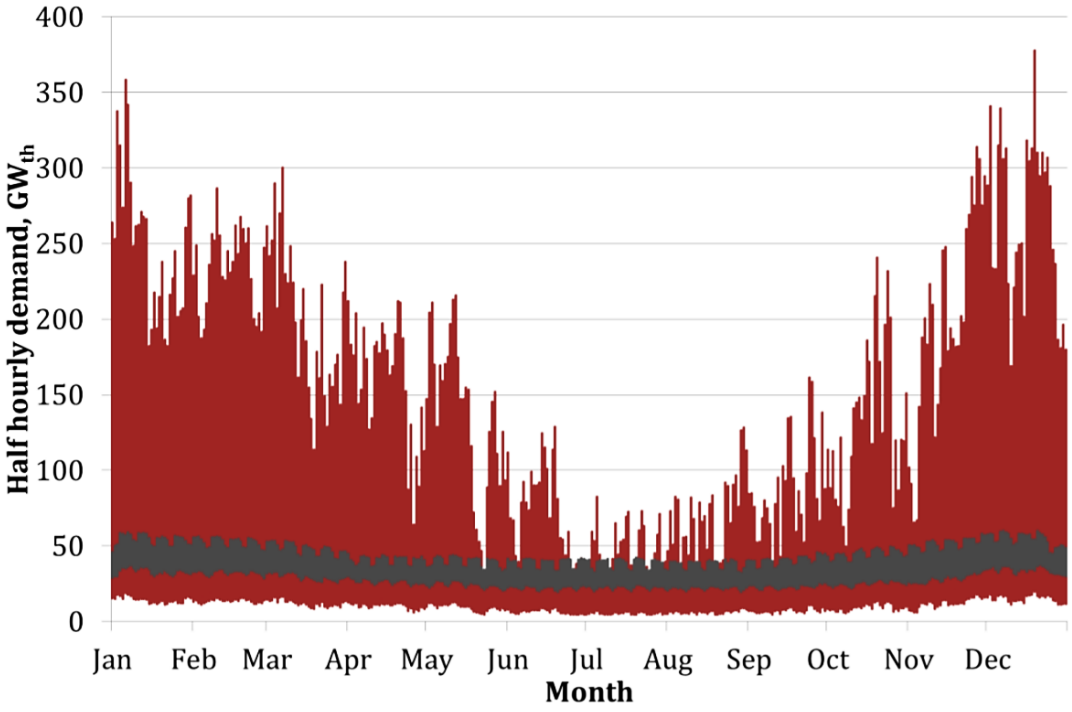

Figure 1. Half-hourly heat demand (red) and electricity demand (grey) in the UK for the year 2010. This chart, made by Sansom (2014), shows the large daily and seasonal fluctuation in demand related to space heating in cold climates and its contrasting magnitude with the electrical grid.

Over the past couple of centuries, underground coal mining has left exceptional hydraulic conditions in the subsurface of thousands of sites, often neighboring metropolitan areas at present (Hall et al., 2011; Menéndez et al., 2019), that regularly allow water extraction rates above 100 $m^3 \cdot h^{-1}$ (Fernandez-Rubio & Lorca, 1993). According to Peralta Ramos et al. (2015), the geothermal potential of such locations has only been exploited in a handful of high-capacity

schemes (> 500 kW) in localities such as Freiberg, Germany; Mieres, Spain; and Heerlen, The Netherlands. However, the low-enthalpy geothermal potential of these shallow sedimentary setting, typically associated with mine-water temperatures well below 30 °C (Figure 2), restricts the performance of ground-source heat pumps (GSHP) and requires the planning of anti-freeze solutions for cases of substantial 'heat mining' in cold environments (Healy & Ugursal, 1997).

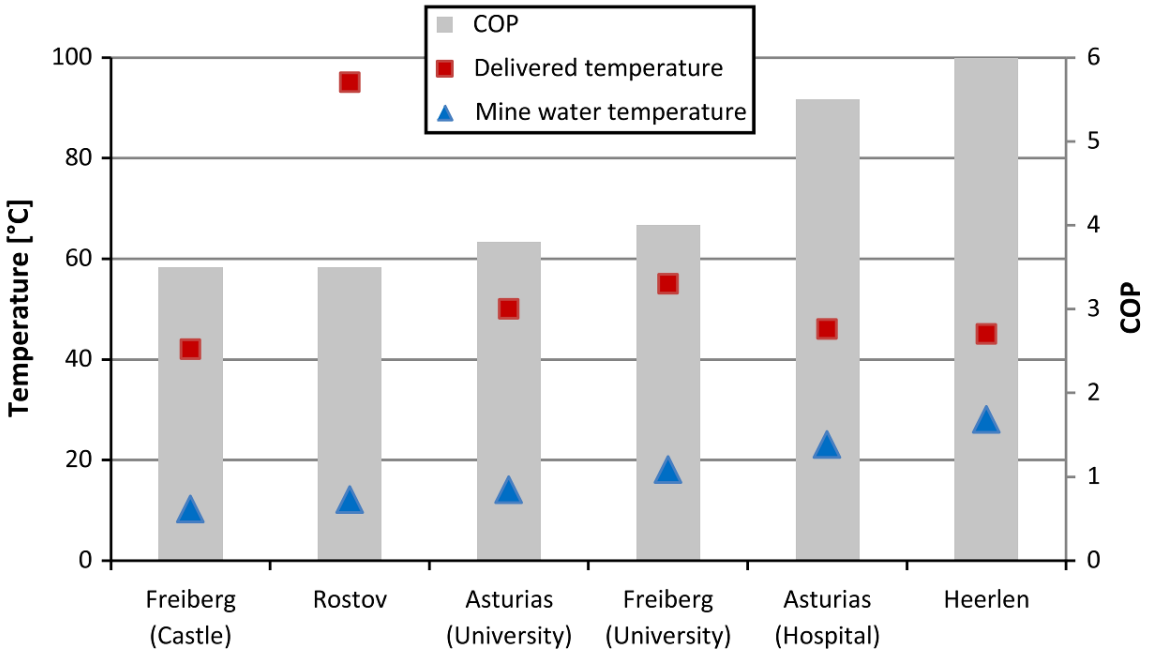

Figure 2. Average mine-water temperature, delivered temperature and Coefficient of Performance (COP) of ground-source heat pumps for large-scale geothermal schemes in legacy coal mines (Peralta Ramos et al., 2015).

To improve the heat extraction efficiency and prevent an early depletion of the geothermal resource, heat harvesting and subsurface storage could be employed using solar thermal collectors or waste heat from domestic/industrial operations, as has been applied in numerous Aquifer Thermal Energy Storage systems (Pellegrini et al., 2019; Fleuchaus et al., 2018). In particular, the third phase of the Heerlen mine-water project (*Minewater 3.0*) incorporates a fifth-generation district heating and cooling system (Figure 3), in which residual heat from a data center, industrial processes, and space cooling is injected to an underground network of four interconnected legacy coal mines functioning as a heat sink (Boesten et al., 2019). The Heerlen project, in operation since October 2008 (*Minewater 1.0*), has resulted in a reduction of around 50% in the CO_2 heat-related intensity in the integrated grid (Behrooz et al., 2008; Verhoeven et al., 2014). Another pioneer scheme in the field is the German HEATSTORE project in the city of Bottrop, where water heated by solar thermal collectors will be injected

into an underground coal mine during summer months, for its extraction during winter to heat the buildings of the International Geothermal Centre (Hahn et al., 2019).

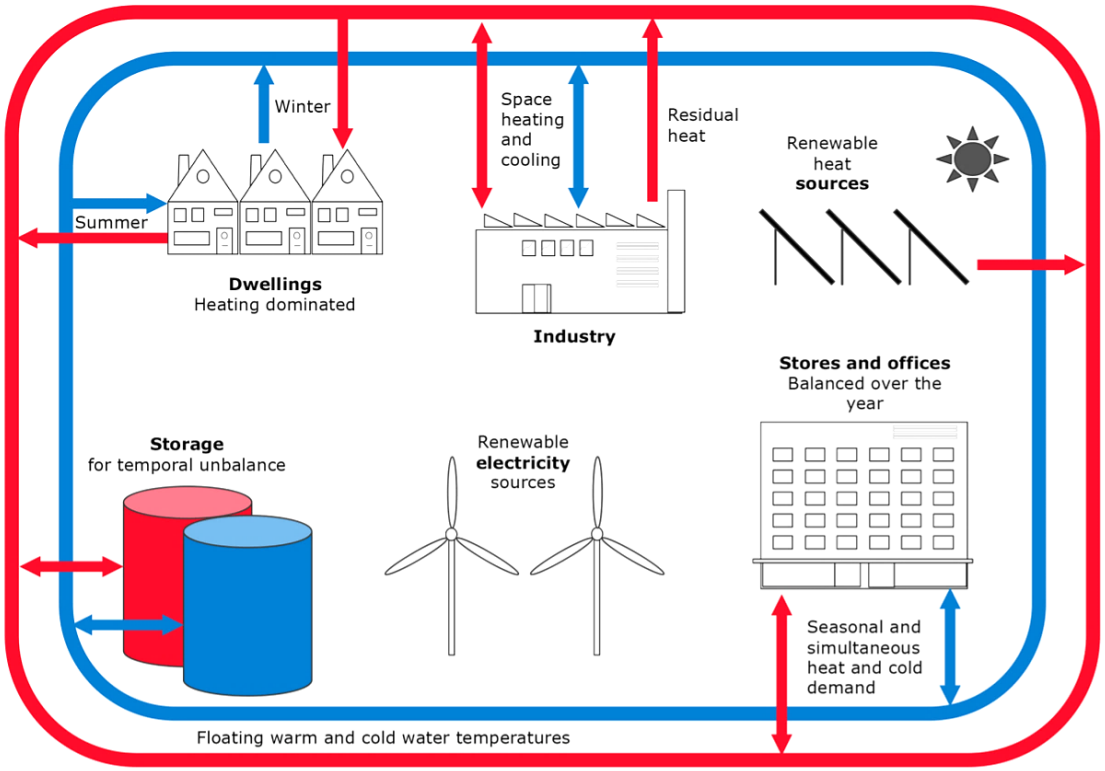

Figure 3. Schematic representation of a fifth-generation district heating system using renewable sources of energy for heat storage (Boesten et al., 2019).

Forecasting the performance of geothermal schemes in legacy coal mines is a complex task due to the variability and frequent inaccuracy in the underground layout, with many mine workings having no official record of existence (Bell & De Bruyn, 1999). Additionally, adverse environmental effects could potentially constrain the exploitation of the geothermal resource, such as acid mine drainage (Banks et al., 1997), hypersaturation of calcite (Jagert et al., 2018) and potential surface uplift due to geomechanical changes (Todd et al., 2019).

Coal, the central lithology in these systems, has an exceptionally low (maceral) matrix thermal conductivity among sedimentary rock, typically ranging from 0.22 to 0.55 $W \cdot m^{-1} \cdot K^{-1}$ (Herrin & Demirig, 1996), that could substantially impact the thermal efficiency in the scheme. The thermal storage capacity (ΔQ) of this lithology under a certain temperature load (ΔT), equation 1, is reduced by the characteristic low bulk density (ρ) of coal despite having a higher specific heat capacity (c) than most for sedimentary rocks – ranging from 1000 to 1400 $J \cdot kg^{-1} \cdot K^{-1}$ (Waples & Waples, 2004; Zhou & Esterle, 2008).

$$\Delta Q = c \rho V \Delta T \qquad (1)$$

The literature review of Loredo et al. (2016) revealed that only a small number of published studies have assessed the geothermal potential of flooded mines through numerical modelling, evidencing the relatively 'unexplored' character of this technique in geoscience. Therefore, as the performance of these geothermal systems has not been extensively analyzed and important shortcomings have been indicated for their numerical simulation (Renz et al., 2009), additional studies are needed to improve the understanding of the subsurface heat transport in coal-rich environments and propose systems adapted to the distinctive geological conditions. In this context, this investigation aims to examine the evolution of a seasonal mine-water heat storage and extraction scheme in generic 3D models of legacy coal extraction panels, addressing critical aspects for its performance, such as:

- How the lithology and porosity of the host rock influence the heat storage capacity in the system.
- The maximum achievable energy retrieval from the subsurface during a heat extraction period with the application of cold-water refill cycles.
- The effect of hydraulic power consumption, associated with water pumping, in the energy balance of the geothermal system.
- A time and financial comparison of the heat recovered from the subsurface with coal and the energy sources presently used for space heating.

2 - Methods

A seasonal layout of two six-month phases, representing a simplification of the typical heat demand of high-latitude regions (Figure 1), was designed for modelling the mine-water thermal scheme of Figure 4. The first phase – heat storage – represents the period of elevated solar intensity and low heat demand around summer months, that would allow the subsurface injection of heated water and transfer of heat to the surrounding rock. Subsequently, water extraction and cold-water reinjection, aimed at retrieving the heat stored in the subsurface with GSHP, would take place to meet the increased space heating demand characteristic of winter months. The modelled storage site corresponds to a generic section of a 2340 m^3 room-and-pillar panel, which is a geometry historically used in mining the shallower coal seams, thus, representative of a sizeable portion of accessible voids in legacy coal mines (Bell & De Bruyn, 1999).

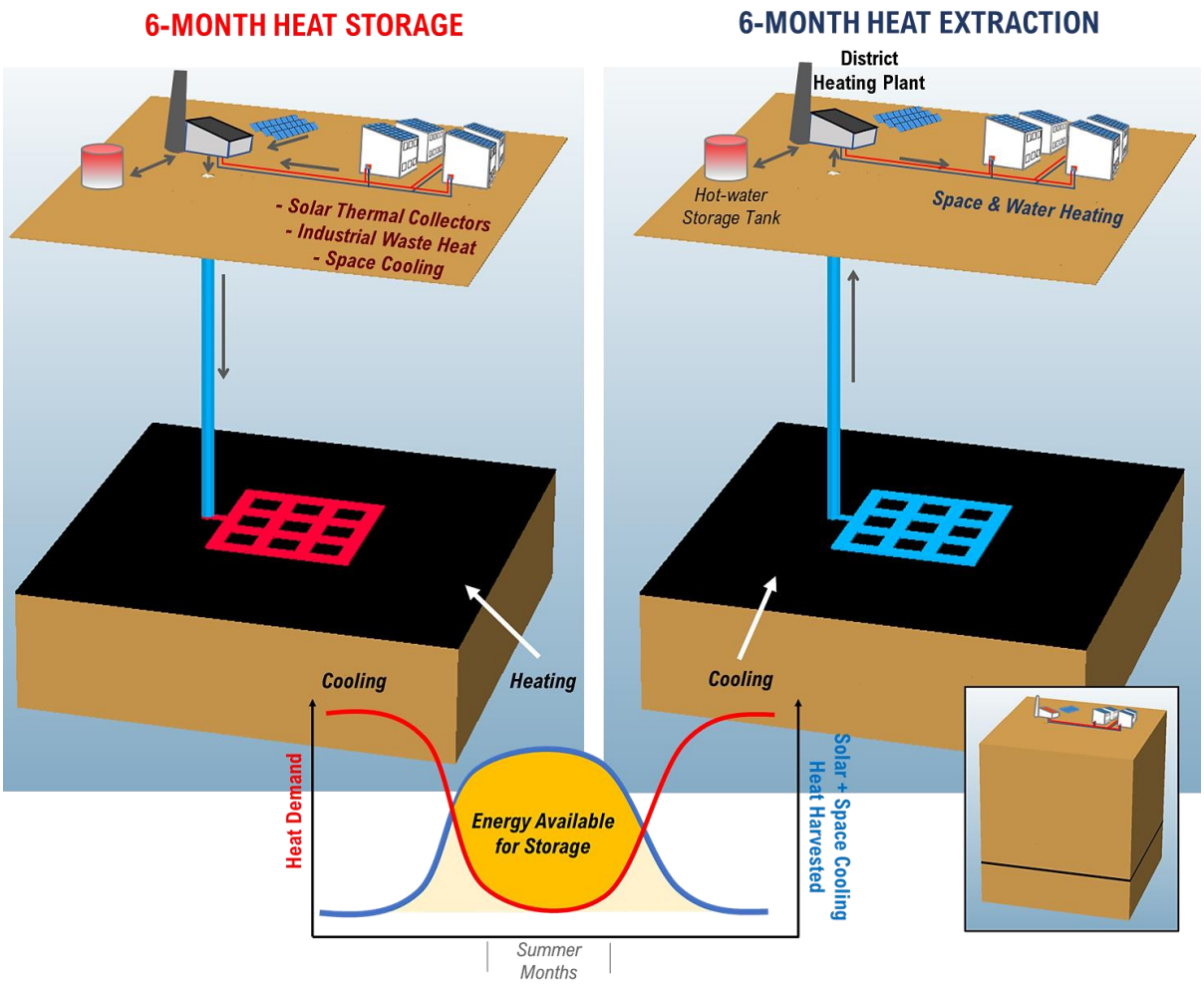

Figure 4. Simplified scheme of the modelled mine-water thermal storage in association with a district heating network. Thermal energy form industrial waste heat, solar thermal collectors or space cooling would be harvested during periods of low heat demand for subsurface storage.

The open-source modelling software *OpenGeoSys* (https://www.opengeosys.org/) is used for the numerical simulations of subsurface heat transport, which applies the Finite Element Method for the approximation and numerical solution of the heat balance partial differential equation. This relationship (2) describes the spatial temperature distribution (*T*) in a porous medium, resulting from the conductive and advective components of heat transport for solid and fluid phases, with a bulk and pore-water density (ρ_s and ρ_w), bulk and pore-water specific heat capacity (c_b *and* c_w), Darcy velocity (*v*), and in the presence of a heat source or sink (*q*). The parameter *D* in this equation corresponds to the bulk thermal diffusivity factor, which is proportional to the thermal conductivity (λ_b) of the porous medium (equation 3).

$$\boldsymbol{D\nabla} \cdot (\boldsymbol{\nabla T}) - \frac{\boldsymbol{c_w \rho_w}}{\boldsymbol{c_b \rho_b}} \boldsymbol{v \nabla^T T} - \boldsymbol{q} = \frac{\boldsymbol{\partial T}}{\boldsymbol{\partial t}} \qquad (2)$$

$$D = \frac{\lambda_b}{\rho_b c_b} \qquad (3)$$

Given the relatively slow movement of groundwater in the subsurface, heat conduction is significantly the dominant thermal mechanism (versus advection) in most sedimentary settings; thus, the thermal properties of rocks-forming minerals have a primary role in subsurface heat transport (Carslaw & Jaeger, 1959). With this in consideration, stationary groundwater conditions are assumed in the models, i.e., no heat advection is modelled or sources of sinks included (q = 0), as a simplification of the heat transport equation that allows more efficient computational processing times of the numerous simulations planned.

As illustrated in Figure 5, a constant surface temperature of 9 °C is set as a (Dirichlet) boundary condition and a moderate geothermal gradient of 0.020 °C·m^{-1} is applied as initial condition, which gives the flooded panel, at a depth of 150 m, an initial temperature of 12 °C. The heat storage phase is simulated with 50 °C constant boundary conditions around the panel, implying the availability of heat sources to maintain a relatively steady thermal state in the mine water. Water extraction and cold-water refills are modelled with a cyclical restart which sets the panel temperature to 12 °C, simulating the complete extraction of the mine-water volume and refill with water at the original geothermal temperature.

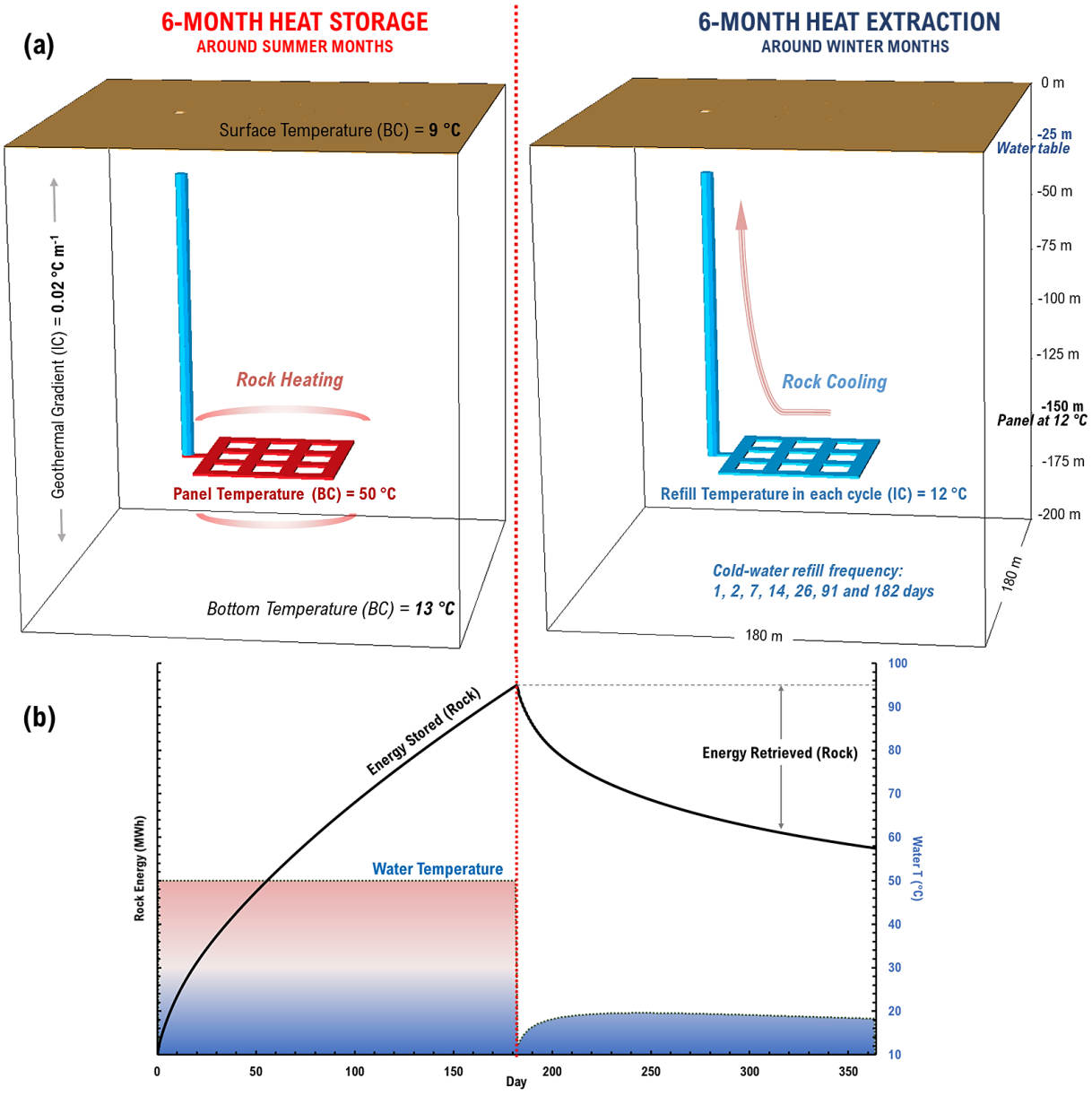

Figure 5. Conceptual model of the heat storage and extraction scheme (a) with the key boundary conditions (BC) and initial conditions (IC) set in *OpenGeoSys*. The energy diagram (b) exemplifies the potential evolution of rock thermal energy and mine-water temperature during an operational year.

Seven different refill intervals are modelled in the heat extraction phase, ranging from 1 to 182 days, to measure the energy recovered from the subsurface with each cycle. Each frequency is proportional to the extraction of a certain volume of water and to a theoretical pumping rate, as shown in Table 1. Periods of one operational year are modelled for all the schemes and a 5-year simulation of the 14-day cycle (of medium efficiency) is conducted to obtain a long-term evolution of the system. Since the modelled instantaneous cold-water refill results in a high heat flux from the host rock towards the mine water (voids), in comparison with a water injection process, the modelling results are representative of the maximum energy that could be retrieved from the rock volume in the heat extraction phase.

Mine-Water Volume	12 °C refill intervals (days)	Total water volume extracted (m³)	Theoretical water pumping rate (m³·h⁻¹)	Theoretical water pumping rate (l·s⁻¹)
2340 m³	1	425880	97.5	27.1
	2	212940	48.8	13.5
	7	60840	13.9	3.9
	14	30420	7.0	1.9
	26	16380	3.8	1.0
	91	4680	1.1	0.3
	182	2340	0.5	0.1

Table 1. Different cold-water refill frequencies modelled in heat extraction phase with the theoretical cumulative water volume extracted for each refill cycle and pumping rate in the 182-day period.

The strong interstratification typically found in coal-bearing sections and uniqueness of the physical properties of coal among sedimentary rocks (Andrés et al., 2016; Wen et al., 2015), can be a challenge for the geothermal simulation of these settings. Coals can habitually display half the density and a sixth of the thermal conductivity of common sedimentary rocks, e.g., sandstones, limestones or shales, whose thermal properties typically overlap (Vasseur et al., 1995; Waples & Waples, 2004). To evaluate this issue, a sensitivity analysis was conducted in a (1 m thick) planar slice of the room-and-pillar panel (Figure 6, 'b'), with a single cold-water refill at the start of the extraction phase and two different host rocks: a typical coal bed and a 'characteristic' sedimentary rock (CSR). The physical (bulk) attributes set to these two materials (density – ρ, thermal conductivity – λ, and specific heat capacity – c) shown in *parameters assigned to the materials in the 3D simulations.

Table 2, were calculated using three porosity (Φ) values and 100% water saturation (equation 4, 5 and 6; Waples & Waples, 2004) to measure the change in the heat storage capacity with an increased pore-water content.

$$\rho_b = \rho_s(1-\Phi) + \rho_f\Phi \qquad (4)$$

$$\lambda_b = \lambda_s(1-\Phi) + \lambda_f\Phi \qquad (5)$$

$$c_b = \frac{[\rho_s c_s(1-\varphi) + \rho_f c_f \varphi]}{\rho_{rock}} \qquad (6)$$

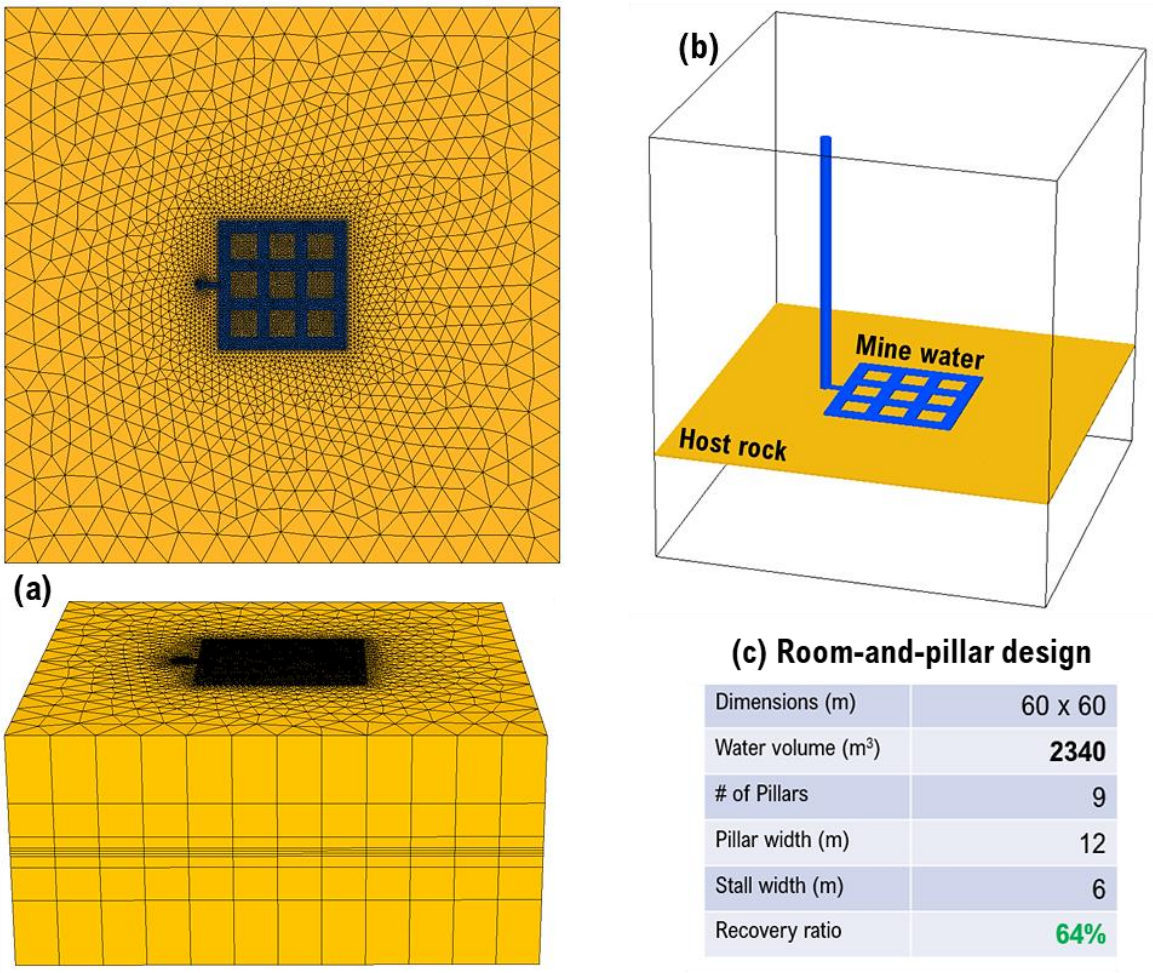

Figure 6. Section of the numerical mesh of prism-shaped elements used in the scheme simulations (a), the panel slice employed in the host-rock sensitivity analysis (b) and spatial dimensions of the 1 m thick generic room-and-pillar panel designed (c).

A simple geological configuration was defined for the storage site (Figure 7), consisting of a single coal layer vertically aligned with the room-and-pillar panel and embedded in a volume of the CSR of ø=0.15 (*parameters assigned to the materials in the 3D simulations.

Table 2). Two models of different coal thickness were used to quantify the effect a minor stratigraphic change would have in the scheme performance; in *Model A,* the 1 m coal layer (same thickness as the panel) puts the mine voids in direct contact with the coal-free rock volume, while in *Model B* the panel is fully embedded by an (exceptionally thick) 3 m coal bed. Since both scenarios can be considered relatively extraordinary for a coal extraction panel, its corresponding simulation results could provide a potential range of heat recovery ratios for the modelled seasonal scheme.

Material		Density ($kg \cdot m^{-3}$)	Specific Heat Capacity ($J \cdot kg^{-1} \cdot K^{-1}$)	Thermal Conductivity ($W \cdot m^{-1} \cdot K^{-1}$)
Water		*1000.0*	*4200.0*	*0.60*
Coal	*Solids*	*1500.0*	*1200.0*	*0.35*
	ø=0.05	1475.0	1301.7	0.36
	ø=0.15*	1425.0	1515.8	0.39
	ø=0.25	1375.0	1745.5	0.41
Characteristic Sedimentary Rock (CSR)	*Solids*	*2650.0*	*800.0*	*3.00*
	ø=0.05	2567.5	866.2	2.88
	ø=0.15*	2402.5	1012.3	2.64
	ø=0.25	2237.5	1179.9	2.40

*parameters assigned to the materials in the 3D simulations.

Table 2. Material properties assigned to the host rock in the six models used for the sensitivity analysis and in the 3D model of the mine-water scheme simulations (parameters also shown in Figure 7).

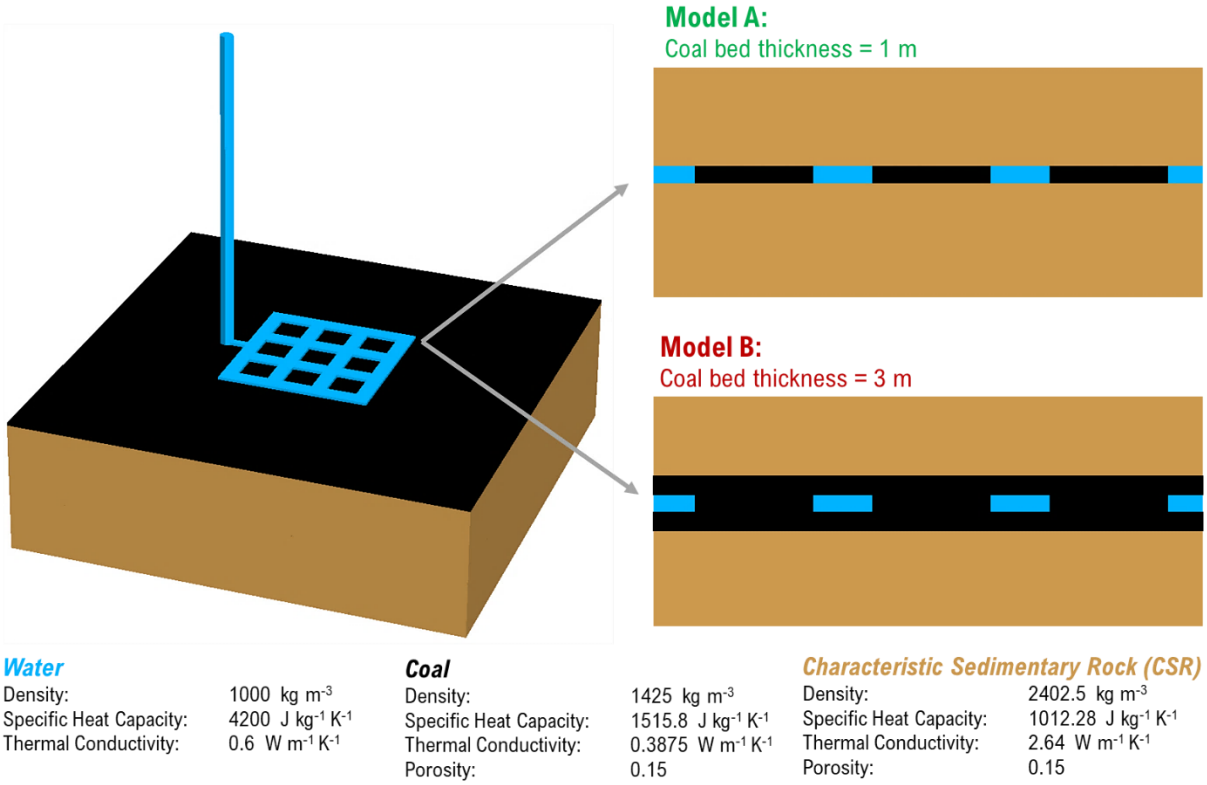

Figure 7. The two geological models and corresponding material properties used in the 3D simulations to investigate the effect that a minor lithological change (coal thickness) has in the performance of the geothermal system.

The thermal energy and average temperature in the rock volume and mine water is measured with daily time-steps for each scheme modelled. Then, after determining the start-end energy difference in the rock volume during the first-year heat extraction phase, indicated as *Energy Retrieved* in Figure 5, the heat retrieval percentage of each refill interval modelled is quantified with equation 7. A recovery of 100% would indicate that all the energy artificially stored in the subsurface was recovered with the cold-water refills; values above 100%, although not modelled in this study, would correspond to 'heat mining' scenarios.

$$Heat\ Retrieval\ \% = \frac{Energy\ Retieved}{Total\ Energy\ Stored} \times 100 \qquad (7)$$

An estimation of the hydraulic power required for the first-year operation of the scheme (equation 8), i.e., energy used in water pumping, was determined using the hypothetical extraction rates of Table 1 (*Q*), a standard value of 0.7 for *Pump Efficiency* (Kaya et al., 2008) and three *Δh* values (25, 75 and 125 m) to investigate the effect of this critical parameter for abandoned mines with a rebounding water table. The *Hydraulic Energy* value is then subtracted from the *Energy Retrieved* to obtain the seasonal *Net-Energy* gain (equation 9), which represents the approximated energy balance in the first operational year of the each scheme modelled.

$$Hydraulic\ Energy = \frac{Q \cdot \Delta h \cdot g \cdot \rho_{water}}{Pump\ Efficiency} \cdot time \qquad (8)$$

$$\boldsymbol{Net\ Energy = Energy\ Retrieved - Hydraulic\ Energy} \qquad (9)$$

The *Net-Energy* values are used in equation 11 to estimate the time it would take for the heat cumulatively recovered from the subsurface to reach the theoretical energy value of the coal 'mined' from the 2340 m^3 of voids. For this, the porosity (ø) and density (ρ) assigned to the coal layer in the 3D numerical model are used in the *Coal Energy* equation (10) and a value of 2.65 $MJ \cdot kg^{-1}$ is used for the *Gross Calorific Value*, which corresponds to the weighted average of all coal consumed in power stations of the UK in 2019 (Department for Business, Energy & Industrial Strategy, 2020). The results of the '*Number of Years'* can be considered a fairly conservative estimation, since a constant first-year scheme performance is assumed and the results of the five-year simulation (Figure 15) confirm that the scheme performance improves annually.

$$Coal\ Energy: Void\ Volume \times (1 - \emptyset) \times \rho_{coal} \times Gross\ Calorific\ Value \qquad (10)$$

$$Number\ of\ Years = \frac{Coal\ Energy}{Net\ Energy} \qquad (11)$$

3 - Results and Discussion

3.1 - *2D Sensitivity Analysis of Thermal Properties*

The temperature distribution maps of Figure 8 illustrate the effect that the modelled material properties change has in the heat storage capacity of the host rocks. A thermal anomaly of smaller extension in the coal scenario, caused by its reduced density and thermal conductivity, is an indication of the lower amount of energy stored in these host-rock models which, subsequently, results in colder mine water during the heat extraction phase. The key role of pillars as heat storage features is also highlighted by the resulting temperature distribution maps; due to their interior location in the panel, these elements constitute a primary source of heat for the cold-water refill in comparison to the peripheral edge of the panel.

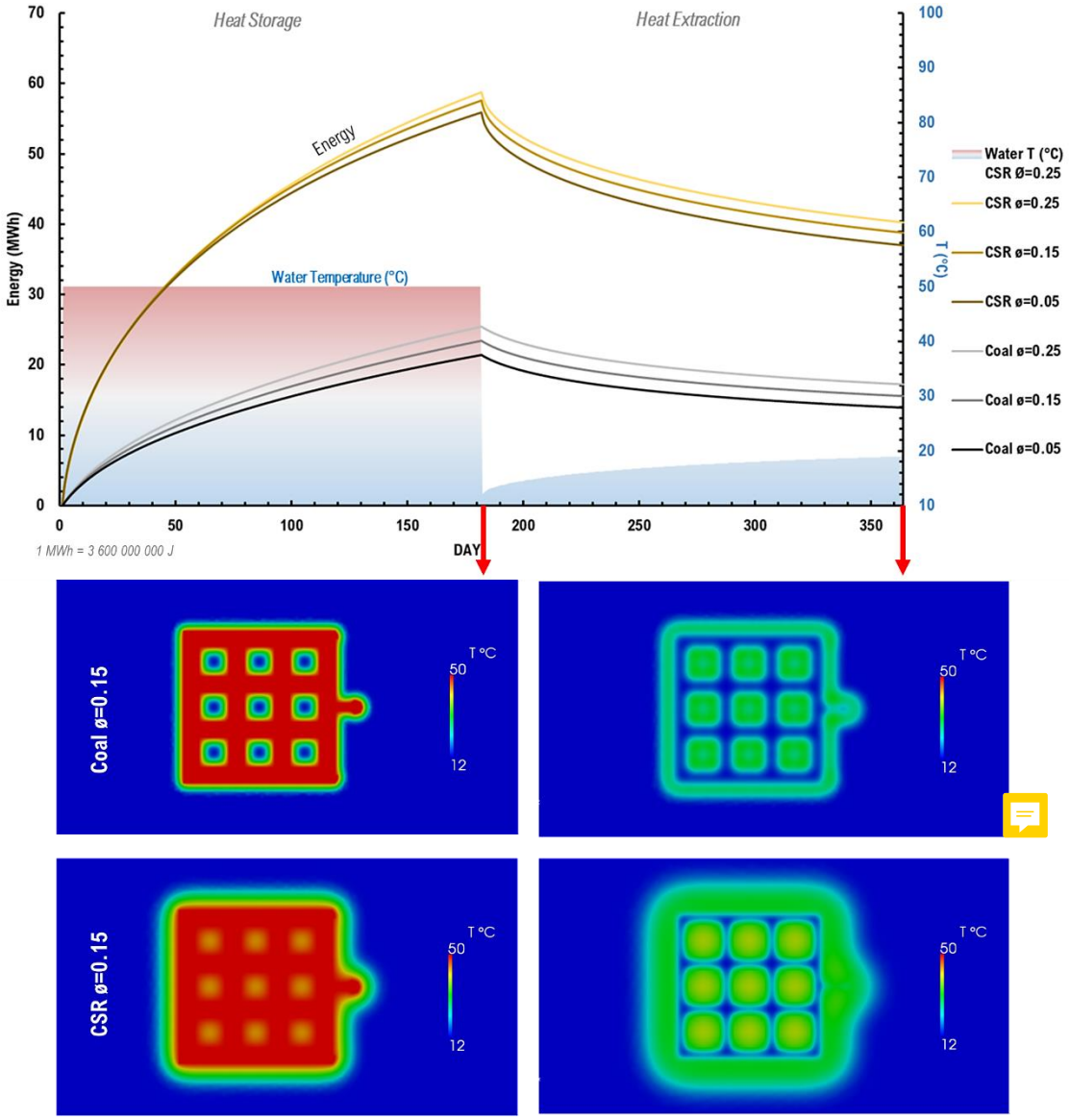

Figure 8. Host-rock energy evolution of the six slices modelled in the sensitivity analysis and referential mine-water temperature of one CSR model. The temperature distribution maps (ø=0.15 scenarios) graphically show the difference in heat transport as a result of the change in thermal properties.

During the modelled initial cycle, more than twice the energy stored in the coal models is acquired by the CSR host rock, as evidenced in Figure 9, largely due to the (~ 1000 kg·m^{-3}) higher rock density in the non-coal scenarios. On the other side, the modelled 5-fold increase in porosity (0.05 - 0.25), which results in higher bulk specific heat capacities, only increases by 16% and 5% the heat stored in the coal and CSR models, respectively. These results evidence the principal role of rock-forming minerals and the smaller influence of pore-water content in the heat storage capacity of the host rocks in these thermal systems, despite the extremely high specific heat capacity of water. However, in the present of a strong groundwater flow, porosity could have a more noticeable effect in heat storage, particularly in panels near thermally conductive lithologies, such as dense sandstones, which would produce large heat distributions zones (as seen in Figure 8) and advective dispersal of heat towards lower hydraulic heads.

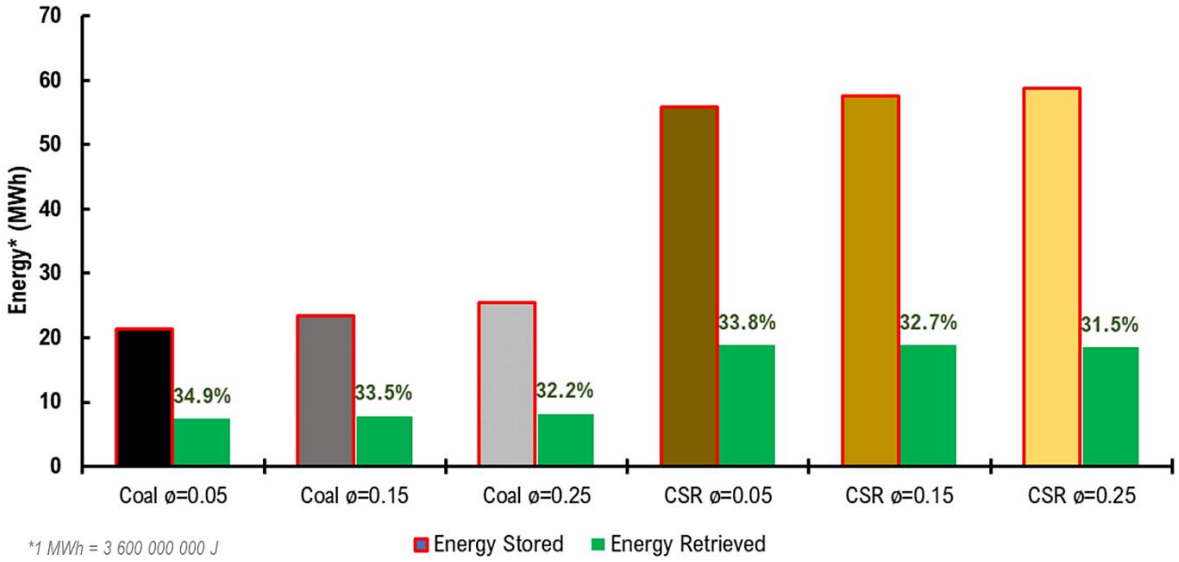

Figure 9. Thermal energy stored and retrieved in the modelled heat storage and extraction phases of the host-rock sensitivity analysis.

3.2 - Mine-Water Thermal Scheme Simulation

The results of the 3D simulations reveal the large impact a small lithological variation and different cold-water refill intervals have in the performance of a mine-water thermal scheme. As evidenced in the graph of Figure 10, 163% more energy is stored in the rock volume of the thin-coal scenario (*Model A*) due to the direct contact with the dense and thermally conductive CSR volume. This considerable increase in stored heat supports the presence of dense strata, e.g., limestones, around mined coal seams as positive features for scenarios of abundant waste heat for harvesting and subsurface injection during summer months. During the first-year heat extraction phase, the energy recovery varies significantly with each refill interval

modelled and, by the end, a substantial amount of energy is still left (unretrieved) in the subsurface even with intensive cycles, as evidenced in the '*Heat Extraction - End*' thermal volume of Figure 12.

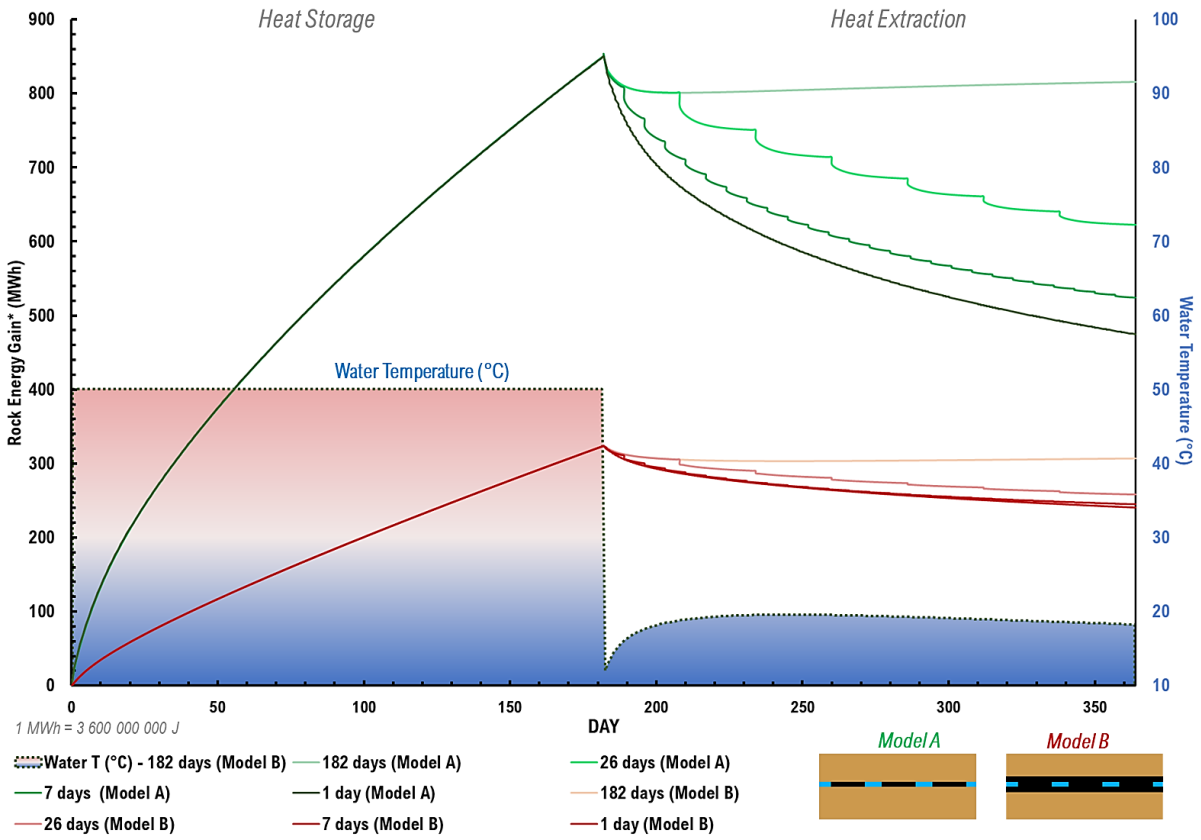

Figure 10. Rock energy evolution in four of the seven refill intervals modelled in the two geological scenarios, with the mine-water temperature of the single-refill cycle of *Model B* used as reference.

As the host rock losses energy with each cold-water refill and the (transient) heat distribution towards the outer edges of the volume progresses, the peak average temperature reached by every consecutive refill gradually declines and a thermal inflection occurs in the single-refill cycle (182 days), Figure 11. This peak temperature point (30.2°C at day 208 for *Model A* and 19.6°C at day 248 in *Model B*), after which the mine water starts to lose energy (heat flux inversion), is delayed in *Model B* due to the insulating effect of the thick embedding coal layer. This condition, albeit unfavorable for the thermal storage capacity of the host rock, prevents temperature loss in the mine water, thus, would suit scenarios of low availability of surplus heat for harvesting and storage.

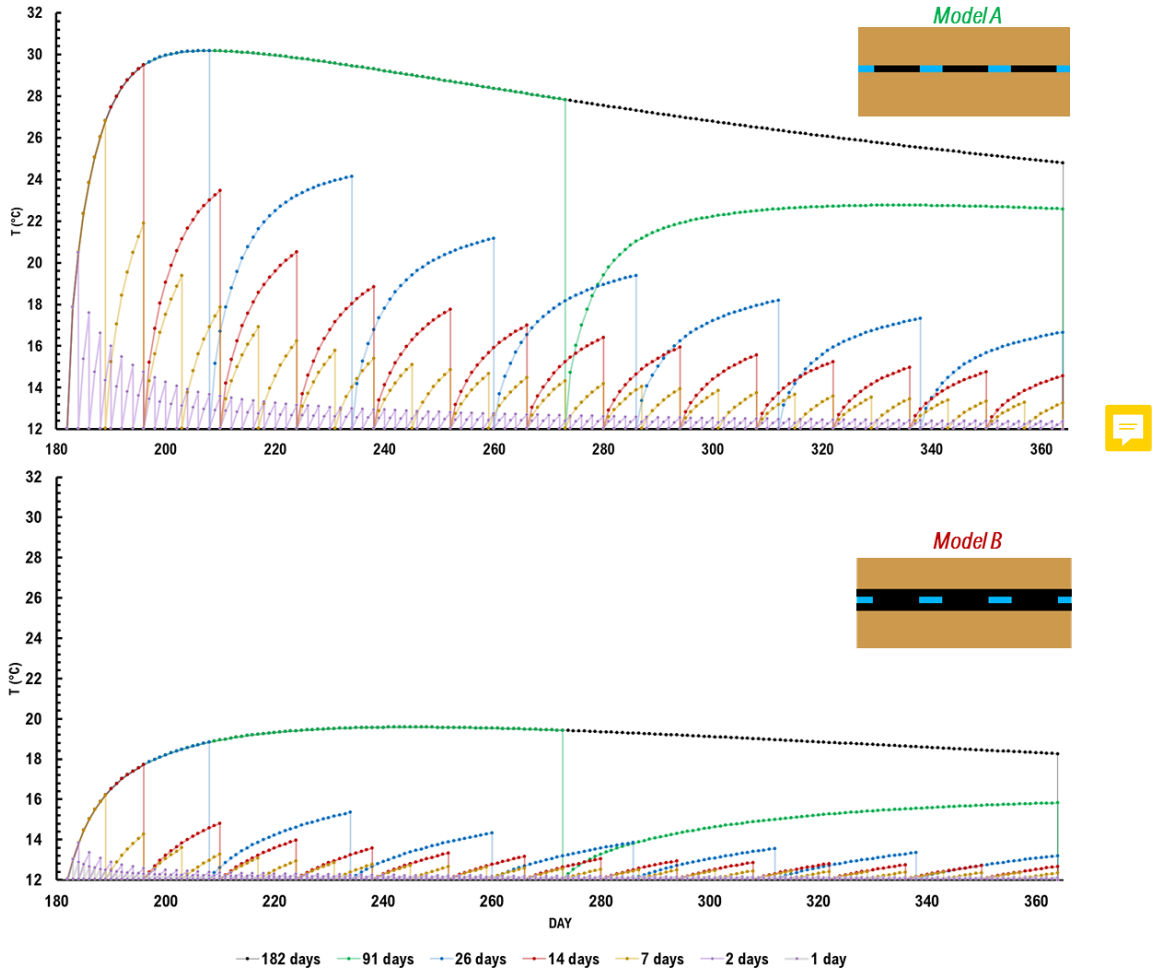

Figure 11. Mine-water temperature evolution in the 6-month heat extraction phase. The vertical lines represent each extraction of the 2340 m^3 volume of water from the panel voids and its refill at 12 °C.

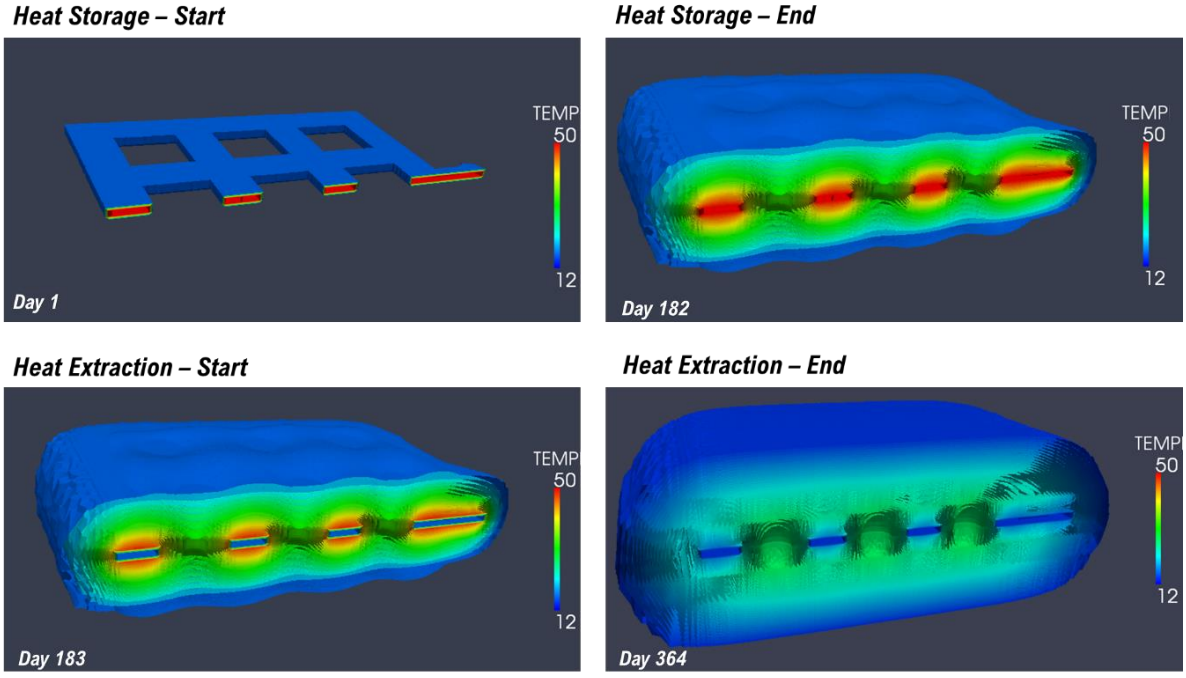

Figure 12. Thermal volumetric contours of the (clipped) room-and-pillar panel at the beginning and end of the first-year heat storage and extraction phases (7-day refill cycle in Model A).

3.3 - Energy Efficiency Assessment

From approximately 25% to 45% of the thermal energy stored in the rock volume during the first heat storage phase, could be recovered in the following six months with optimized water refill cycles at the original geothermal temperature. While a higher heat recovery is achieved with shorter refill intervals, which counter the heat dispersal outside the storage panel, the deceleration observed at higher frequencies points to a practical limit in the maximum achievable heat recovery (Figure 13). As this magnitude is exclusively controlled by conductive heat transport in the numerical models, it is lower for *Model B* where the thick coal layer reduces the heat flux towards the cold-water refill and causes an earlier plateau in the heat recovery percentage. In single-refill scenario (182 days), the heat recovery, of around 5%, is lower than the values obtained in the 2D sensitivity analysis (~ 33%) due the unchanged pillar area (main thermal source) and a substantial increase in the peripheral panel area in the 3D model, which has a lower heat contribution to the cold-water refill.

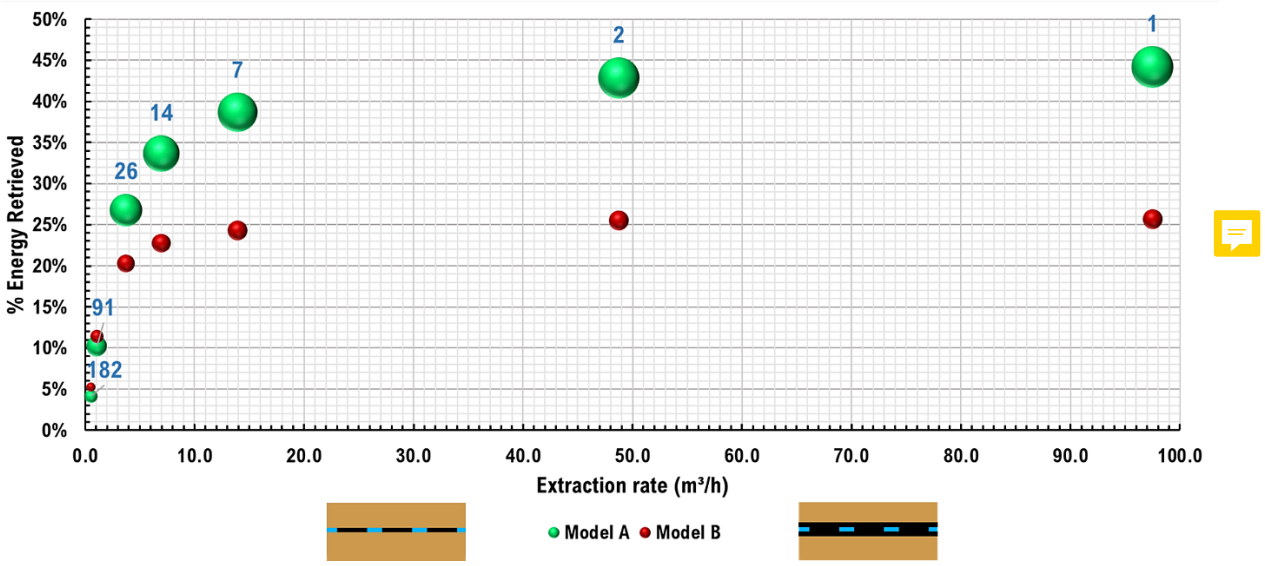

Figure 13. Percentage of heat recovered from the subsurface in the first-year heat extraction phase for the refill modelled intervals. The bubble area represents the amount of energy extracted in each scenario.

Since elevated mine-water circulation (refill cycles) entails a higher energy consumption in water pumping (*1 MWh = 3 600 000 000 J*

Table 3), the *Net-Energy* gain from the geothermal scheme is strongly reduced in the most intensive cycles. As shown in Figure 14, the hydraulic power requirements could substantially alter the energy yield in the system and produce a negative energy balance for large pumping rates. This adverse outcome is observed in *Model B* for the largest water extraction rates and deeper water-table scenarios, where more energy would be consumed in pumping operations than cumulatively extracted from the subsurface. Should the GSHP thermal boost documented in existing mine-water geothermal projects (Figure 2) be applied to these results, no scenario

in the modelled scheme would produce a negative energy balance, even in the deepest water table cases (125 m).

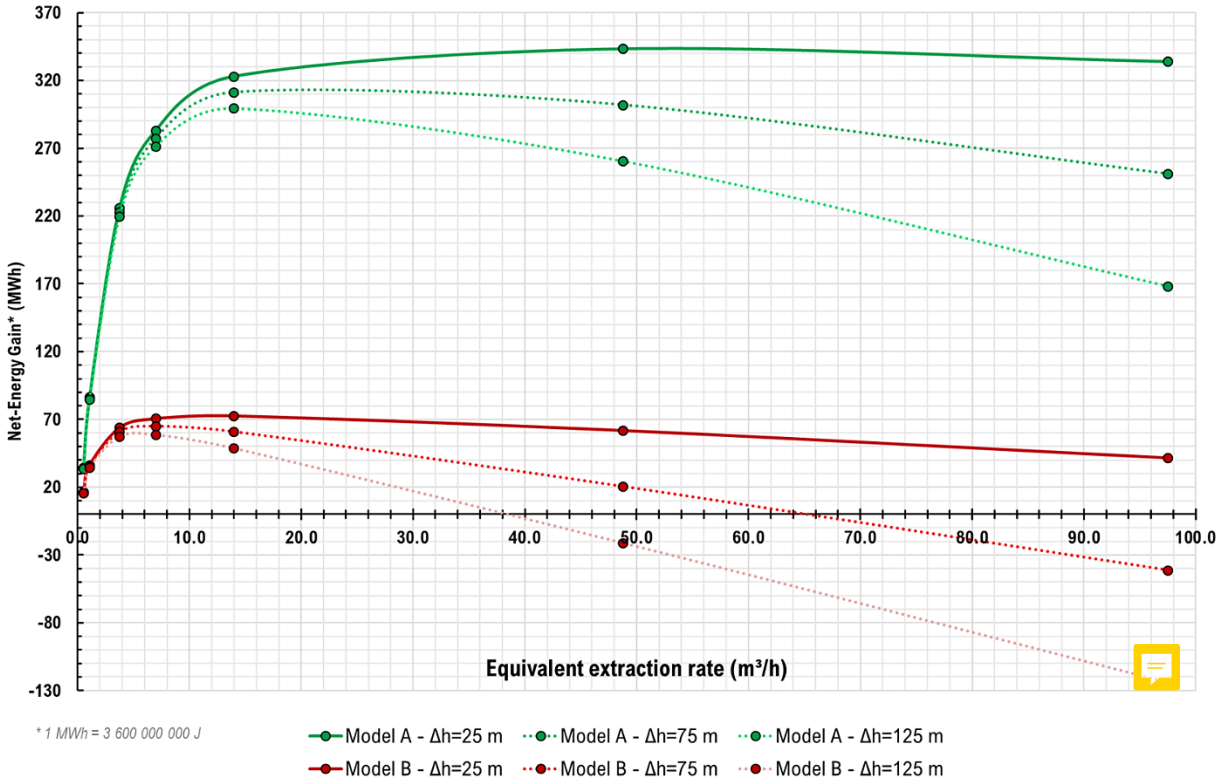

Figure 14. *Net-Energy* recovery of each refill cycle in its equivalent extraction rate. This parameter takes into account the hydraulic power consumption in water pumping for the three Δh evaluated.

Scenario	Refill cycle (Days)	m3/h	ΔEnergy - Stored (MWh)	Energy Recovered (MWh)	% Energy Recovery	Hydraulic Energy Δh= 25 m (MWh)	Net-Energy Δh= 25 m (MWh)
Model A	1	97.5	850.2	375.5	44.2%	41.4	**334.0**
	2	48.8	850.2	364.2	42.8%	20.7	**343.4**
	7	13.9	850.2	329.0	38.7%	5.9	**323.1**
	14	7.0	850.2	286.0	33.6%	3.0	**283.0**
	26	3.8	850.2	227.8	26.8%	1.6	**226.2**
	91	1.1	850.2	86.8	10.2%	0.5	**86.4**
	182	0.5	850.2	34.8	4.1%	0.2	**34.6**
Model B	1	97.5	323.5	83.1	25.7%	41.4	**41.7**
	2	48.8	323.5	82.6	25.5%	20.7	**61.9**
	7	13.9	323.5	78.6	24.3%	5.9	**72.7**
	14	7.0	323.5	73.7	22.8%	3.0	**70.7**
	26	3.8	323.5	65.6	20.3%	1.6	**64.0**
	91	1.1	323.5	36.8	11.4%	0.5	**36.4**
	182	0.5	323.5	17.0	5.3%	0.2	**16.8**

1 MWh = 3 600 000 000 J

Table 3. Energy results of the 3D scheme simulation (first year) for the two modelled geological scenarios with a Δh= 25 m.

3.4 - Long-term scheme operation

As evidenced in the five-year simulation of a medium-efficiency refill cycle (Figure 15), the yearly temperature growth in the subsurface results in an increased thermal contrast with the cold-water refills, during the heat extraction phase, which improves the scheme efficiency progressively (Table 4). The percentage increase diminishes as the transient conditions in the geothermal system approach a quasi-steady state and the system evolves into a relative thermal equilibrium with the seasonal thermal input. After three years, the energy retrieved surpasses 50% of the heat seasonally stored in the modelled medium-efficiency scenario, as a consequence of the gradual establishment of the heat reservoir in the subsurface by the long-term thermal 'charge' given to the rock volume.

Year	Energy - end of storage phase	Energy - end of extraction phase	ΔEnergy in Host-Rock (storage)	Energy recovered from rock (extraction)	% Energy Recovery	% Increase
1	850.2	564.2	850.2	286.0	**33.6%**	-
2	1301.1	973.5	737.0	327.7	**44.5%**	**10.8%**
3	1670.3	1324.6	696.9	345.8	**49.6%**	**5.2%**
4	2000.3	1643.7	675.7	356.5	**52.8%**	**3.1%**
5	2306.0	1942.2	662.2	363.8	**54.9%**	**2.2%**

**Energy in MWh (1 MWh = 3 600 000 000 J)*

Table 4. Energy results of the five-year simulation for the 14-day cold-water refill cycle in *Model A*.

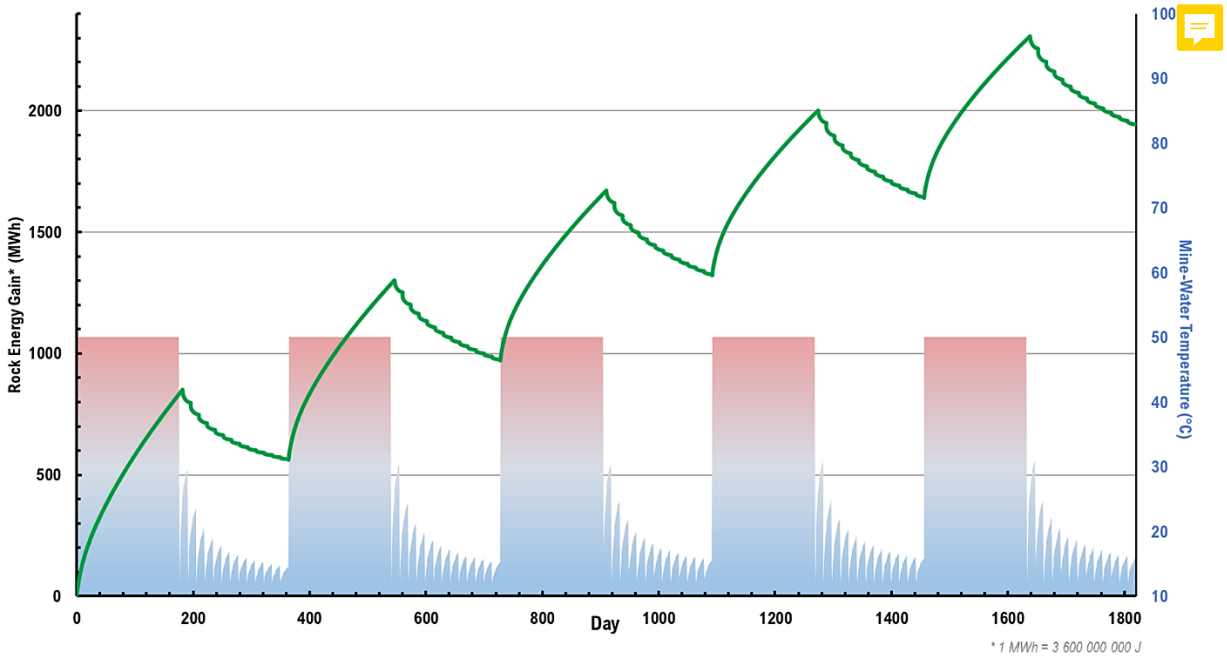

Figure 15. Thermal energy evolution in the rock volume (green) and mine-water temperature (color-shaded) for the five-year simulation of the 14-day refill cycle in *Model A*.

3.5 - Coal Energy Analysis

Assuming a constant first-year *Net-Energy* yield in the mine-water geothermal scheme, which the five-year simulation confirms as a conservative hypothesis, it is be possible to attain the 21961.9 MWh of (theoretical) energy in the 2983.5 t of 'mined' coal in less than 80 years of scheme operation, in favorable geological settings and optimized water extraction cycles. A broad interpretation of the results of Figure 16 points to the 100 - 300 years range as an easily-attained timespan for the cumulative heat recovered to reach the gross calorific value of the coal extracted from the voids. Although the *Number of Years* estimation is representative of the modelled 50 °C storage, 12 °C cold-water refills, hydraulic power consumption associated with a Δh of 25 m, and include the modelling simplifications mentioned in the *Methods* section, it offers a general perspective of how this low-enthalpy geothermal option compares to coal, a historically source of energy that is intrinsically connected to the mine-water scheme.

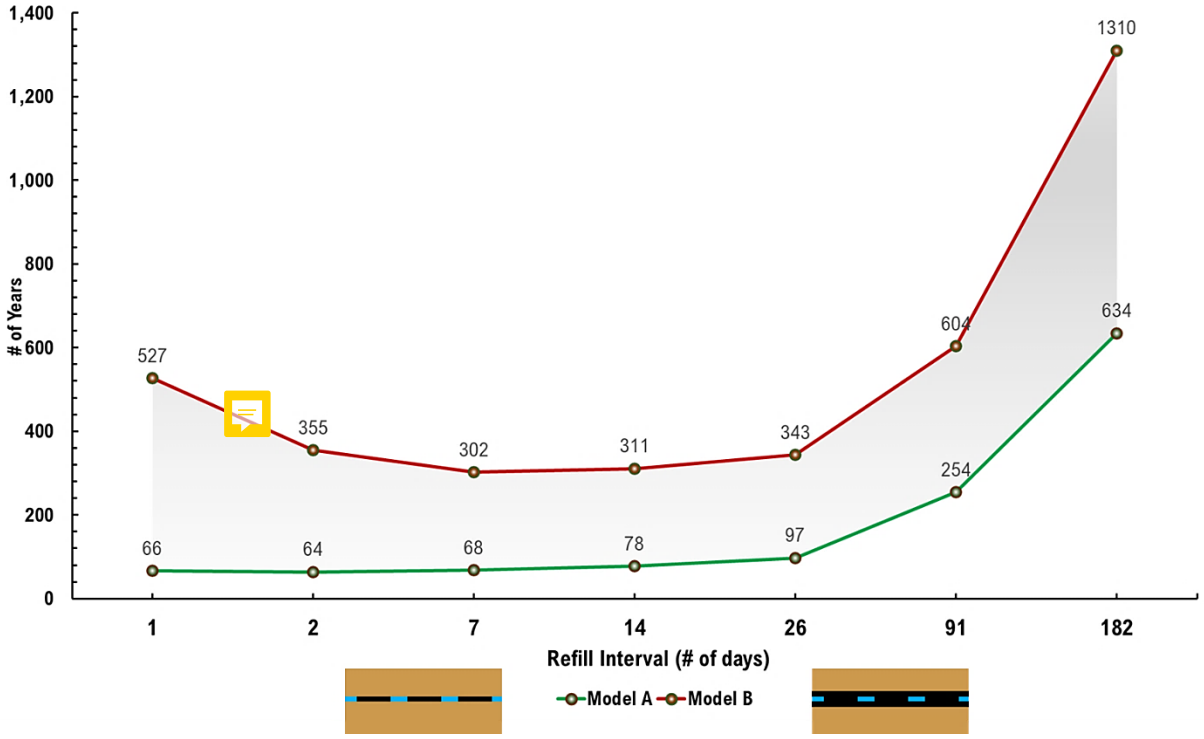

Figure 16. Number of years for the cumulative *Net-Energy* obtained in each modelled scheme to reach the theoretical energy of the 'mined' coal in the 3D model, assuming a constant first-year performance.

Finally, the basic financial analysis of Figure 17 aims to associate the heat retrieved from the scheme to the energy value of natural gas and electricity, the most frequently used alternatives for heating at present. With information from the UK Department for Business, Energy & Industrial Strategy (2020) the hypothetical market value of the 2983.5 t of mined coal was estimated using the five-year average (2015 - 2019) of adjusted price per kWh of all coal purchased by major power producers in the country. Similarly, the value of energy unit for

electricity and natural gas (£·kWh^{-1}) was estimated using the 5-year average price (2015 - 2019) purchased by non-domestic consumers in the UK. Then, the monetary value of the seasonal *Net-Energy* recovered in the 14-day refill cycle (283 MWh) – medium efficiency scenario, again conservatively assuming a constant first-year performance, could equal the worth of the 'mined' coal in 5.4 years using electricity prices, and in 25.3 years using gas prices, i.e., assigning a high and low price to the energy recovered, respectively. If the positive system evolution observed in the 5-year simulation is considered, the straightforward financial analysis could show an even more favorable outlook for this seasonal heat storage technology.

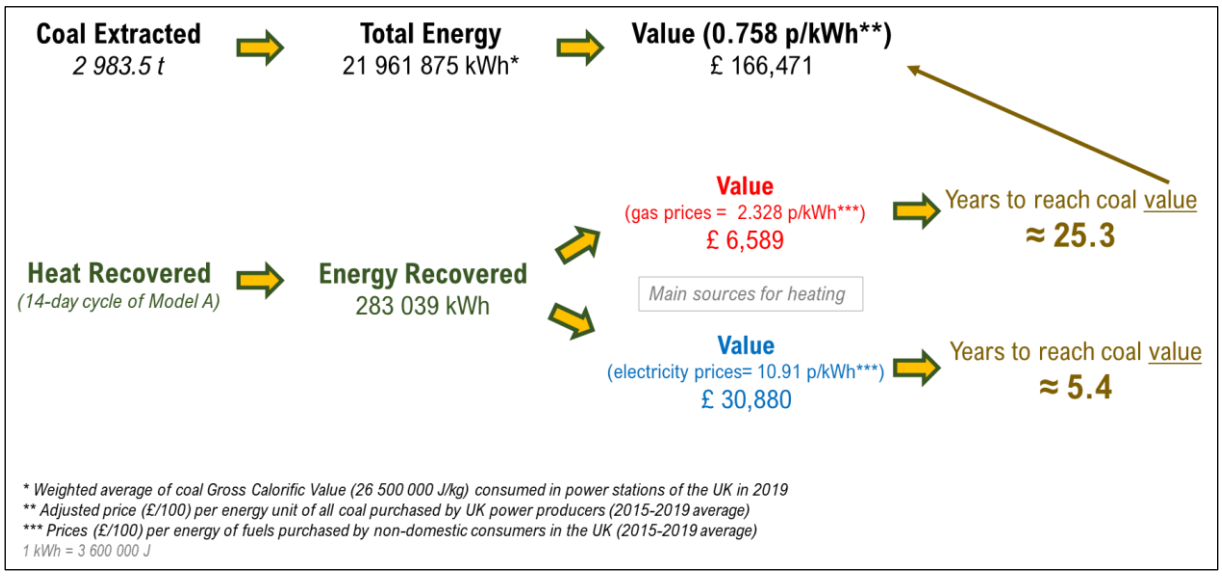

Figure 17. Basic financial comparison of the worth of the 'mined' coal in the 3D model with the heat recovered in the first heat extraction phase of the 14-day refill cycle in *Model A*. For the 'Years to reach coal value' calculation, a constant first-year heat recovery is assumed. Energy statistics source: UK Department for Business, Energy & Industrial Strategy (2020).

4 - Conclusion and Recommendations

The results of this modelling study demonstrate that the efficiency of seasonal thermal storage in coal mines is highly dependent on the site geology and design of heat extraction cycles. In absence of a significant groundwater flow, rock-forming minerals have a much larger influence than pore-water content in the heat storage capacity of host rocks. Simple lithological variations, such as the modelled 2 m difference in coal thickness, could result in a 2-fold increase of energy transferred to the subsurface in a six-month heat storage period. In room-and-pillar panels, pillars are a primary source of heat for the injected water due to their inner-structure location; therefore, their geometry in plans of abandoned mines should be carefully evaluated for determining prospective sites. The presence of thermally conductive strata around these panels, such as dense sandstones, promotes the establishment of a thermal reservoir in the subsurface and could substantially increase the heat recovery percentage.

In the first operational year, up to 45% of the energy transferred to the subsurface, in a six-month heat storage phase, could be retrieved by cold-water circulation in the mine voids during the following six months. The long-term simulation of a conservative scenario shows that the energy recovery could easily exceed 50% in the first five years of operation, due to the transient thermal growth in the subsurface produced by the seasonal thermal input. These transient conditions and the heat flux from the host rock should be evaluated when designing the cold-water circulation, since an energy recovery plateau could occur at large pumping rates that might produce a negative energy balance in the system for extremely adverse scenarios.

It could be possible to reach the energy of the ‘mined’ coal in less than 80 years of scheme operation by optimizing the heat extraction cycles. A broader interpretation of the results points to the 100 - 300 years period as a feasible timespan to reach the theoretical coal energy. In financial terms, the cumulative heat recovered could equal the market value of the ‘mined’ coal in less than 10 years with an optimized cold-water circulation and favorable energy prices. Although aspects such as the temperature boost of ground-source heat pumps, the role of coal inter-stratification and advective heat transport (coupled thermo-hydraulic modelling) should be included for a more comprehensive assessment in future modelling studies, the results of this investigation demonstrate the value these subsurface voids have for the diversification of the heat sector in the current decarbonization context.

Funding

This research did not receive any specific grant from funding agencies in the public, commercial, or not-for-profit sectors.

References

Andrés, C., Álvarez, R., & Ordóñez, A. (2016). Estimation of thermal conductivity of rocks from their mineralogical composition (Asturian Coal Basin, NW Spain) for modelling purposes. *Environmental Earth Sciences*, *75*(3), 1–10. https://doi.org/10.1007/s12665-015-5037-8

Banks, D., Younger, P. L., Arnesen, R. T., Iversen, E. R., & Banks, S. B. (1997). Mine-water chemistry: The good, the bad and the ugly. *Environmental Geology*, *32*(3), 157–174. https://doi.org/10.1007/s002540050204

Behrooz, B. S., Elianna, D., & Jan-Jaap, V. B. (2008). Geothermal Use of Deeop Flooded Mines. *Post-Mining 2008*, *July*, 1–11.

Bell, F. G., & De Bruyn, I. A. (1999). Subsidence problems due to abandoned pillar workinqs in coal seams. *Bulletin of Engineering Geology and the Environment*, *57*(3), 225–237. https://doi.org/10.1007/s100640050040

Bertermann, D., Klug, H., & Morper-Busch, L. (2015). A pan-European planning basis for estimating the very shallow geothermal energy potentials. *Renewable Energy*, *75*, 335–347. https://doi.org/10.1016/j.renene.2014.09.033

Boesten, S., Ivens, W., Dekker, S. C., & Eijdems, H. (2019). 5Th Generation District Heating and Cooling Systems As a Solution for Renewable Urban Thermal Energy Supply. *Advances in Geosciences*, *49*, 129–136. https://doi.org/10.5194/adgeo-49-129-2019

Carslaw, H. S., & Jaeger, J. C., (1959) Conduction of Heat in Solids, second edition, Oxford University Press, Oxford, UK, 310.

Dahash, A., Ochs, F., Janetti, M. B., & Streicher, W. (2019). Advances in seasonal thermal energy storage for solar district heating applications: A critical review on large-scale hot-water tank and pit thermal energy storage systems. *Applied Energy*, *239*(December 2018), 296–315. https://doi.org/10.1016/j.apenergy.2019.01.189

Department for Business, Energy & Industrial Strategy (2020). Calorific values of fuels. Digest of UK Energy Statistics. https://www.gov.uk/government/statistics/dukes-calorific-values

Department for Business, Energy & Industrial Strategy (2020). Average prices of fuels purchased by the major UK power producers. https://assets.publishing.service.gov.uk/government/uploads/system/uploads/attachment_data/file/947035/table_321.xlsx

Department for Business, Energy & Industrial Strategy (2020). Prices of fuels purchased by non-domestic consumers in the UK. https://assets.publishing.service.gov.uk/government/uploads/system/uploads/attachment_data/file/947037/table_341.xlsx

Dodds, P. E., & Demoullin, S. (2013). Conversion of the UK gas system to transport hydrogen. *International Journal of Hydrogen Energy*, *38*(18), 7189–7200.

https://doi.org/10.1016/j.ijhydene.2013.03.070

Fernandez-Rubio, R., & Lorca, D. F. (1993). Mine water drainage. *Mine Water and the Environment*, *12*(1), 107–130. https://doi.org/10.1007/BF02914803

Fleuchaus, P., Godschalk, B., Stober, I., & Blum, P. (2018). Worldwide application of aquifer thermal energy storage – A review. *Renewable and Sustainable Energy Reviews*, *94*(July), 861–876. https://doi.org/10.1016/j.rser.2018.06.057

Hahn, F., Jagert, F., Bussmann, G., Nardini, I., Bracke, R., Seidel, T., & König, T. (2019). *The reuse of the former Markgraf II colliery as a mine thermal energy storage Injection of surplus heat Production of stored heat*. *June*, 11–14.

Hall, A., Scott, J. A., & Shang, H. (2011). Geothermal energy recovery from underground mines. *Renewable and Sustainable Energy Reviews*, *15*(2), 916–924. https://doi.org/10.1016/j.rser.2010.11.007

Healy, R. F., & Ugursal, V. L. (1997). Performance and economic feasibility of ground source heat pumps in cold inmate. *International Journal of Energy Research*, *21*(10), 857–870. https://doi.org/10.1002/(sici)1099-114x(199708)21:10<857::aid-er279>3.3.co;2-t

Herrin, J. M., & Demirig, D. (1996). Thermal conductivity of U . S . coals Subbituminous Coal Lignite Bituminous Coal. *Journal of Geophysical Research*, *101*, 381–386.

Jagert, F., Hahn, F., Ignacy, R., Bussmann, G., & Bracke, R. (2018). Mine water of abandoned coal mines for geothermal heat storage : Hydrogeochemical modeling and predictions. *11th ICARD IMWA Conference*. https://www.imwa.info/docs/imwa_2018/IMWA2018_Jagert_375.pdf

Kaya, D., Yagmur, E. A., Yigit, K. S., Kilic, F. C., Eren, A. S., & Celik, C. (2008). Energy efficiency in pumps. *Energy Conversion and Management*, *49*(6), 1662–1673. https://doi.org/10.1016/j.enconman.2007.11.010

Loredo, C., Roqueñí, N., & Ordóñez, A. (2016). Modelling flow and heat transfer in flooded mines for geothermal energy use: A review. *International Journal of Coal Geology*, *164*, 115–122. https://doi.org/10.1016/j.coal.2016.04.013

Lund, J. W., & Boyd, T. L. (2016). Direct utilization of geothermal energy 2015 worldwide review. *Geothermics*, *60*, 66–93. https://doi.org/10.1016/j.geothermics.2015.11.004

Menéndez, J., Ordóñez, A., Álvarez, R., & Loredo, J. (2019). Energy from closed mines: Underground energy storage and geothermal applications. *Renewable and Sustainable Energy Reviews*, *108*(April), 498–512. https://doi.org/10.1016/j.rser.2019.04.007

Pellegrini, M., Bloemendal, M., Hoekstra, N., Spaak, G., Andreu Gallego, A., Rodriguez Comins, J., Grotenhuis, T., Picone, S., Murrell, A. J., & Steeman, H. J. (2019). Low carbon heating and cooling by combining various technologies with Aquifer Thermal Energy Storage. *Science of the Total Environment*, *665*, 1–10. https://doi.org/10.1016/j.scitotenv.2019.01.135

Peralta Ramos, E., Breede, K., & Falcone, G. (2015). Geothermal heat recovery from abandoned

mines: a systematic review of projects implemented worldwide and a methodology for screening new projects. *Environmental Earth Sciences*, *73*(11), 6783–6795. https://doi.org/10.1007/s12665-015-4285-y

REN21. (2019). *Renewables 2019 Global Status Report.* Paris: REN21 Secretariat). ISBN 978-3-9818911-7-1. http://www.ren21.net/Portals/97/documents/GSR/REN21_GSR2011.pdf

Renz, A., Rühaak, W., Schätzl, P., & Diersch, H. J. G. (2009). Numerical modeling of geothermal use of mine water: Challenges and examples. *Mine Water and the Environment*, *28*(1), 2–14. https://doi.org/10.1007/s10230-008-0063-3

Sansom, R. (2014). Decarbonising low grade heat for low carbon future. *Imperial College London*, *October*. https://spiral.imperial.ac.uk/bitstream/10044/1/25503/1/Sansom-R-2015-PhD-Thesis.pdf

Sayegh, M. A., Danielewicz, J., Nannou, T., Miniewicz, M., Jadwiszczak, P., Piekarska, K., & Jouhara, H. (2017). Trends of European research and development in district heating technologies. *Renewable and Sustainable Energy Reviews*, *68*, 1183–1192. https://doi.org/10.1016/j.rser.2016.02.023

Todd, F., McDermott, C., Harris, A. F., Bond, A., & Gilfillan, S. (2019). Coupled hydraulic and mechanical model of surface uplift due to mine water rebound: Implications for mine water heating and cooling schemes. *Scottish Journal of Geology*, *55*(2), 124–133. https://doi.org/10.1144/sjg2018-028

Vasseur, G., Brigaud, F., & Demongodin, L. (1995). Thermal conductivity estimation in sedimentary basins. *Tectonophysics*, *244*(1–3), 167–174. https://doi.org/10.1016/0040-1951(94)00225-X

Verhoeven, R., Willems, E., Harcouët-Menou, V., De Boever, E., Hiddes, L., Veld, P. O. t., & Demollin, E. (2014). Minewater 2.0 project in Heerlen the Netherlands: Transformation of a geothermal mine water pilot project into a full scale hybrid sustainable energy infrastructure for heating and cooling. *Energy Procedia*, *46*(December 2014), 58–67. https://doi.org/10.1016/j.egypro.2014.01.158

Waples, D. W., & Waples, J. S. (2004). A review and evaluation of specific heat capacities of rocks, minerals, and subsurface fluids. Part 2: Fluids and porous rocks. *Natural Resources Research*, *13*(2), 123–130. https://doi.org/10.1023/B:NARR.0000032648.15016.49

Watson, S. D., Lomas, K. J., & Buswell, R. A. (2019). Decarbonising domestic heating: What is the peak GB demand? *Energy Policy*, *126*(December 2018), 533–544. https://doi.org/10.1016/j.enpol.2018.11.001

Wen, H., Lu, J. H., Xiao, Y., & Deng, J. (2015). Temperature dependence of thermal conductivity, diffusion and specific heat capacity for coal and rocks from coalfield. *Thermochimica Acta*, *619*, 41–47. https://doi.org/10.1016/j.tca.2015.09.018

Zhou, B., & Esterle, J. (2008). Toward improved coal density estimation from geophysical logs. *Exploration Geophysics*, *39*(2), 124–132. https://doi.org/10.1071/EG08011